Oxygen aggregation kinetics, thermal donors and carbon-oxygen defect formation in silicon containing carbon and tin

Angeletos, T. , Sgourou, E.N. , Andrianakis, A. , Diamantopoulou, A. , Chroneos, A. and Londos, C.A.

AIP Journal of Applied Physics

Oxygen aggregation kinetics, thermal donors and carbon-oxygen defect formation in silicon containing carbon and tin

T. Angeletos, E. N. Sgourou, A. Andrianakis, A. Diamantopoulou, A. Chroneos, and C. A. Londos

Citation: Journal of Applied Physics **118**, 015704 (2015); doi: 10.1063/1.4923388
View online: http://dx.doi.org/10.1063/1.4923388
View Table of Contents: http://scitation.aip.org/content/aip/journal/jap/118/1?ver=pdfcov
Published by the AIP Publishing

Oxygen aggregation kinetics, thermal donors and carbon-oxygen defect formation in silicon containing carbon and tin

T. Angeletos,[1] E. N. Sgourou,[1] A. Andrianakis,[1] A. Diamantopoulou,[1] A. Chroneos,[2,3] and C. A. Londos[1]
[1]*Solid State Section, Physics Department, University of Athens, Panepistimiopolis, Zografos, 157 84 Athens, Greece*
[2]*Faculty of Engineering and Computing, Coventry University, Priory Street, Coventry CV1 5FB, United Kingdom*
[3]*Department of Materials, Imperial College London, London SW7 2BP, United Kingdom*

(Received 21 May 2015; accepted 22 June 2015; published online 2 July 2015)

Localized vibrational mode spectroscopy measurements on Czochralski silicon (Cz-Si) samples subjected to isothermal annealing at 450 °C are reported. First, we studied the effect of carbon (C) and tin (Sn) isovalent dopants on the aggregation kinetics of oxygen. It is determined that the reduction rate of oxygen is described by the Johnson-Mehl-Avrami equation in accordance with previous reports. The activation energy related with the reaction rate constant of the process is calculated to increase from Cz-Si, to C-doped Cz-Si (CCz-Si), to Sn-doped Cz-Si contained C (SnCz-Si). This is attributed to the presence of the isovalent dopants that may impact both the kinetics of the oxygen atoms and also may lead to the formation of other oxygen-related clusters. Second, we studied the effect of Sn on the formation and evolution of carbon-oxygen (C-O) defects. It was determined that the presence of Sn suppresses the formation of the C-O defects as indicated by the reduction in the strength of the 683, 626, and 586 cm^{-1} well-known bands of C_sO_i defect. The phenomenon is attributed to the association of Sn with C atoms that may prevent the pairing of O with C. Third, we investigated the effect of C and Sn on the formation of thermal donors (TDs). Regarding carbon our results verified previous reports that carbon suppresses the formation of TDs. Interestingly, when both C and Sn are present in Si, very weak bands of TDs were observed, although it is known that Sn alone suppress their formation. This may be attributed to the competing strains of C and Sn in the Si lattice. © *2015 AIP Publishing LLC*.
[http://dx.doi.org/10.1063/1.4923388]

I. INTRODUCTION

Oxygen is the most dominant impurity unintentionally introduced in Si during crystal growth. It is incorporated in the lattice mostly at interstitial sites (O_i) and is present in complexes with other impurities such as carbon in Si. Cz-Si material is saturated with oxygen at the melting temperature and therefore it becomes supersaturated at lower temperatures resulting in an inhomogeneous distribution of oxygen in the material. Subsequently, for technological purposes it is important to homogenise the oxygen in Si making it suitable for device fabrication. To this end, thermal processing of the material is required. On thermal treatments, at above 350 °C[1–17] the oxygen atoms become mobile and begin to aggregate forming oxygen clusters, which exhibit double donor behaviour. These defects are well known as thermal donors (TDs). There are families of such donors depending on the temperature of the treatment. The first family of TDs is formed in the temperature range 350–500 °C comprising of small aggregates of oxygen atoms, being the early stage of oxygen precipitation. The formation of thermal donors affects the electrical properties of Si and therefore, it is critical to know in detail their properties and behaviour in order to suppress their harmful effects on devices. Consequently, their formation was studied intensively and extensively both experimentally and theoretically in the last sixty years.[1–17] Infrared (IR) absorption bands in the wavenumber spectral ranges 575–580 cm^{-1}, 720–750 cm^{-1}, and 975–1015 cm^{-1} have been reported in the literature. They have been correlated with the first stage of the oxygen aggregation process in Si initiated by the formation of oxygen dimers following with structures comprising a larger number of oxygen atoms being attached during the thermal treatments.[18–25]

Carbon is the other main impurity in Si, besides oxygen, unintentionally added in the lattice during growth. Being a group IV element, carbon is incorporated at substitutional sites (C_s) and is electrically neutral. Due to its small size carbon atoms can preferentially provide sites in their neighbourhood for oxygen atoms. These sites serve in essence as nucleation sites for oxygen aggregation.[26] Notably, in Cz-Si with high carbon concentration, C_sO_i complexes are formed after heat treatments and can be been detected by IR spectroscopy even in as grown Si. Three satellite bands labelled as X, Y, and Z at 586, 637, and 684 cm^{-1}, respectively, has been correlated with vibration modes of the C_sO_i defect.[3,27,28] Furthermore, it is well known that the presence of carbon suppresses the formation of TDs in Si.[3,29] It has been suggested[30,31] that this suppression is due to the competing process of the interaction of oxygen and carbon atoms to form carbon-oxygen complexes. Notably, measurements of the evolution of the carbon and loss from the solution

upon annealing at 450 °C in carbon contained Cz-Si showed that two O_i atoms are removed for each C_s atom and a band at 1026 cm^{-1} has been attributed to a C-O_2 complex.[3,32,33] In an alternative explanation[34,35] the suppression of thermal donors due to the presence of carbon was attributed to the release of silicon self-interstitials (Si_I) which has been postulated as involved in the generation process of TDs. C atoms react strongly with Si_I reducing their concentration leading finally to a reduction of the TDs formation. Studies of the kinetics of TDs generation have shown that in the course of their formation also dissociation as well as transformation to electrically inactive centres occurs. The latter processes were found to be affected by the presence of C, leading to the suppression of TDs.[36,37] In another approach, the suppression of TDs in C containing Cz-Si has been related to the effect of strains introduced in the Si lattice by C atoms. The latter impurities being smaller than that of Si atoms, which replace at substitutional sites introduce tensile strains which tend to compensate the compressive strains due to the larger oxygen atoms at interstitial sites. As a result, the impulse for oxygen agglomeration is weakened leading to a reduction in TDs formation.[29,38,39] Importantly, although the effect of C on the formation of TDs can be realised and understood with different models and points of consideration the picture is not complete mainly because the exact configuration of TDs is not completely known.[40]

Among the various techniques used to control TDs formation in Si, improving the quality of the material for device fabrication, is isovalent doping. Sn is a group IV element, as is the carbon impurity. It is incorporated in the Si lattice at substitutional sites and is electrically neutral. Sn has a covalent radius $r_{Sn} = 1.41$ Å which is larger than that of Si ($r_{Si} = 1.17$ Å). It introduces compresses strains in the lattice acting as an effective trap for vacancies (V).[41,42] On the other hand, C having a covalent radius $r_C = 0.77$ Å acts as an effective trap for Si_I. It has been reported[43,44] that Sn-doped n-type Si suppresses the formation of TDs, although other work reported[45] no effect on TDs for p-type Sn-doped Si. In order to explain the role of Sn in the reduction of the TDs, it was suggested[44] that metastable O-Sn complexes are formed. As a result, the availability of oxygen atoms in the oxygen agglomeration process is reduced leading to a suppression of the TDs formation. Alternatively, it was suggested[43] that the strains induced in the lattice due to the incorporation at substitutional sites of the larger than Si Sn atoms led to a reduction of the capture probability of the oxygen atom by an oxygen-related complex to finally form a TD structure. Notably, the reduction in the formation of TDs in Ge-doped Si was attributed[46] to the strains introduced by the Ge atoms in the Si lattice, which cause an increase of the energy barrier related with the aggregation of oxygen atoms. This could reduce the quasi-equilibrium concentrations of the oxygen complexes[47] suppressing finally the formation of the TDs. We can extend this reasoning to the case of Sn-doped Si where the even larger covalent radius of Sn results in larger induced strains eventually resulting to a lower generation of TDs.

As we mentioned above device fabrication processes on Si-based material involve heat treatments. Such treatments at 450 °C result in the formation of thermal donors. This formation is affected by the presence of C and Sn. Both impurities suppress the generation of TDs, although with different mechanisms in each case. The aim of this work is to study the effect of the simultaneous present of high C and Sn on the generation of TDs in Si. This is particular interesting, due to the fact that C and Sn affect differently the intrinsic defects, since C affects the Si_I and Sn the V. Thus, a combination of both impurities in the Si lattice is expected to have a significant impact on device performance. Notably, the issue of the combined effect of C and Sn in Si was highlighted earlier.[48] It was considered as a potential technological tool from the viewpoint of the radiation hardness of Si material.

II. EXPERIMENTAL DETAILS

In this work, we used three groups of mechanically polished Cz samples of ~2 mm thickness doped with C and/or with Sn. In particular one Cz-Si sample with carbon concentration below detection limit, one CCz-Si sample contained C and one SnCz-Si sample contained Sn. The latter sample contained also C of about the same order as the CCz-Si sample. All the samples were n-type with a phosphorous concentration of $\sim 10^{15}$ cm^{-3}. The Sn concentration was determined by secondary ion mass spectrometry (SIMS) and the value was given by the provider. The oxygen and the carbon concentrations of the samples were calculated from the 1106 cm^{-1} oxygen IR band and the 606 cm^{-1} carbon band, using calibration coefficients of 3.14×10^{17} cm^{-2} for oxygen and 1×10^{17} cm^{-2} for carbon, respectively.[49,50] Details of the samples used are given in Table I.

The samples were subjected to a series of isothermal anneals at 450 °C of 8 h duration each. After each annealing step the IR measurements were carried out at room temperature by using a Fourier Transform IR (FTIR) spectrometer operating at a resolution of 1 cm^{-1}. The two phonon intrinsic absorption was always removed by subtracting the spectrum of a Float zone sample of equal thickness.

III. RESULTS AND DISCUSSION

A. Kinetics of oxygen aggregation at 450 °C

Fig. 1 shows the evolution of O_i versus time for the isothermal anneal at 450 °C. Now the reduction ratio of interstitial oxygen is defined[51] by the expression

$$y = [O_i(0) - O_i(t)]/[O_i(0) - O_s], \quad (1)$$

where $O_i(t)$ and O_s are the oxygen concentration at time t and the solid solubility of oxygen, respectively. The oxygen solubility at a temperature T is given[52] by the expression

TABLE I. Oxygen, carbon and tin concentration of the samples used in the present study.

Samples	[Sn] 10^{18}(cm^{-3})	$[O_i]_o$ 10^{18}(cm^{-3})	$[C_s]_o$ 10^{18}(cm^{-3})
Cz-Si	…	1.34	…
CCz-Si	…	1.03	1.36
SnCz-Si	9	0.97	0.94

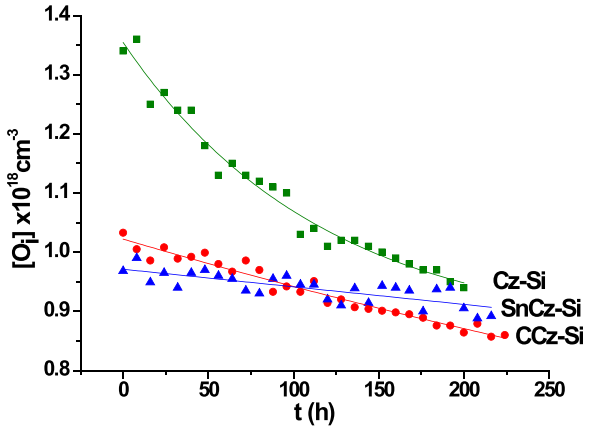

FIG. 1. The evolution of O_i versus annealing time at 450 °C for the Cz-Si, CCz-Si, and SnCz-Si samples.

$$O_s = 3.24 \times 10^{21} \exp(-1.03\,\mathrm{eV}/k_B T)\mathrm{atoms/cm}^3. \quad (2)$$

In the 450–650 °C temperature range the reduction ratio y of oxygen versus time t obeys the Johnson-Mehl-Avrami (JMA) equation[51]

$$y = 1 - \exp[-(kt)^n], \quad (3)$$

where n and k are the time exponent and the reaction rate constant. The value of n normally ranges from 0.5 to 2.5, and can be used conveniently to classify reactions according to their kinetics.[53] Fig. 2 exhibits the plot of $[\ln\cdot\ln(1-y)^{-1}]$ versus [ln t(min)] for our data, indicating that there is a linear relation between these two quantities. According to the Eq. (3) the corresponding slope of the straight line is equal to n and the interception with the vertical axis is equal to $n\cdot\ln k$. The values of n and k, determined from Fig. 2 for each of the three samples, are reported in the Table II.

We observe that the reaction rate k becomes smaller in C-doped Cz-Si and even smaller in Sn-doped Cz-Si containing carbon. Regarding the parameter n specifying the time exponent in Eq. (3) we observe that in C-doped Cz-Si it has a value of about the same as in Cz-Si, although it is reduced in the case of Sn-doped Si. We notice that the values of n are equal to 0.78 and 0.77 for carbon-free material (Cz-Si) and carbon-rich material (CCz-Si), respectively, being in essence very

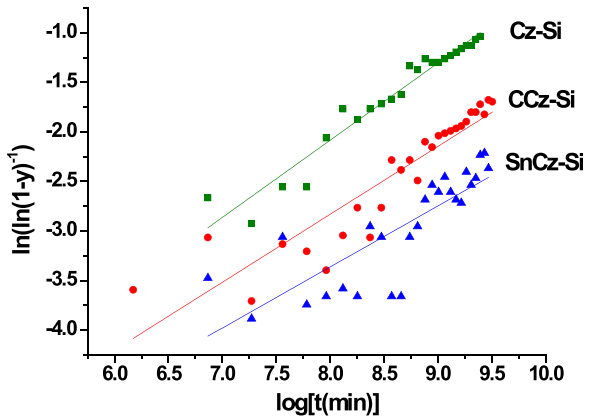

FIG. 2. Plot of $[\log\cdot\log(1-y)^{-1}]$ versus [log t(min)], for the Cz-Si, CCz-Si, and SnCz-Si samples.

TABLE II. Values of n, k, and λ for the samples used in the present study.

Sample	n	k ($\times10^{-6}$ min^{-1})	λ ($\times10^{-38}$ h·cm^2)$^{-1}$
Cz-Si	0.78	23.3	0.14
CCz-Si	0.77	7.56	0.09
SnCz-Si	0.62	1.43	0.05

close to the value of $n = 0.73$ reported previously[51] for isothermal treatments at 450 °C. However, in the case of Sn-doped Cz-Si it is $n = 0.62$. The later value is similar to the value of 0.60 reported[51] for treatments at 500 °C. Notably, n was reported[51] to decrease between 450 and 500 °C. Arguably, the effect of Sn on the nucleation kinetics of oxygen at 450 °C is comparable with the effect of the increase of the isothermal anneal temperature from 450 to 500 °C in Cz-Si.

Furthermore, the reaction ratio k is given by the expression

$$k = k_o \exp(-E_g/k_B T)\mathrm{cm}^{-1}, \quad (4)$$

where E_g is the activation energy of k. By applying Eq. (4) for the case of CCz-Si and SnCz-Si and taking the ratio of the two corresponding relations we receive

$$k_{CCz}/k_{SnCz} = (k_{CCz})_o/(k_{SnCz})_o \cdot \exp[(E_{g\,SnCz} - E_{g\,CCz})/k_B T)]. \quad (5)$$

Now assuming[51] that $(k_{CCz})_o \approx (k_{SnCz})_o$, we have

$$E_{g\,SnCz} - E_{g\,CCz} = k_B T \cdot \ln(k_{CCz}/k_{SnCz}). \quad (6)$$

As we see from Table II, $k_{CCz} > k_{SnCz}$ and therefore, $E_{g\,SnCz} > E_{g\,CCz}$. Similarly, we can conclude that $k_{Cz} > k_{CCz}$. The results indicate that the activation energy E_g of the reaction rate increases from Cz-Si to CCz-Si to SnCz-Si. This can be attributed to the introduction of the isovalent dopants in the lattice that impact the kinetics of the oxygen atoms and the formation of oxygen related clusters.[44,54–58] Notably, it has been determined that Sn reduces the activation energy of oxygen diffusion in Si.[44]

One expects that the time exponent n and the activation energy E_g to exhibit opposite trends, that is, the increase of one is associated with the decrease of the other. In order to show that we combine Eqs. (3) and (4) to express n as a function of E_g. First, we notice that in the temperature range of 450–650 °C, O_s which can be found from Eq. (2) has values of 10^{14}–10^{15} cm^{-3} which are around three order of magnitude smaller than the oxygen concentration of the samples used in this experiment. Thus, O_s can be neglected. Therefore, Eqs. (1) and (3) can be written, respectively, as follows:

$$y = [O_i(0) - O_i(t)]/[O_i(0) - O_s] \approx 1 - O_i(t)/O_i(0) \quad (7)$$

$$\text{and} \quad O_i(t) = O_i(0)\exp[-(kt)^n]. \quad (8)$$

By taking the logarithm of Eq. (8) and replacing k from Eq. (4), we obtain

$$\ln(O_i(0)/O_i(t)) = (tk_o)^n \exp(-E_g/k_B T). \quad (9)$$

Considering two samples, specified by (E_{g1}, n_1) and (E_{g2}, n_2), respectively, by Eq. (9), we obtain:

$$\ln(O_i(0)_1/O_i(t)_1)/\ln(O_i(0)_2/O_i(t)_2) = (tk_o)^{n1-n2}\exp[-(n_1E_{g1}-n_2E_{g2})/k_BT)], \quad (10)$$

where $O_i(0)_1$, $O_i(t)_1$ and $O_i(0)_2$, $O_i(t)_2$ are the corresponding concentrations of O_i at the beginning of anneals and at annealing time t.

Let us define c by the following expression:

$$c = [\ln(O_i(0)_1/O_i(t)_1)/\ln(O_i(0)_2/O_i(t)_2)]/[(tk_o)^{n1}\exp(-n_1E_{g1}/k_BT)]. \quad (11)$$

Apparently, c is always positive because the ratios $O_i(0)_1/O_i(t)_1$ and $O_i(0)_2/O_i(t)_2$ are greater than 1.

Therefore, Eq. (10) can be written as

$$c = (tk_o)^{-n2}\exp(n_2E_{g2}/k_BT) > 0 \quad (12)$$

and by taking its logarithm we have

$$n_2 = \ln c/[(E_{g2}/k_BT) + \ln(tk_o)]. \quad (13)$$

Therefore, the activation energy E_g increases, as the parameter n decreases. In our case the values of n cited in Table II show that n decreases from Cz-Si to CCz-Si to SnCz-Si, although the activation energies E_g show an opposite trend as reported above.

The kinetic equation that govern the evolution of oxygen versus time[51] upon isothermal anneals at 450 °C has the expression

$$dO_i(t)/dt = -\lambda \cdot O_i(t)^3. \quad (14)$$

Upon solving this equation, we have the relation

$$[O_i(0)/O_i(t)]^2 - 1 = 2\lambda t O_i(t)^2. \quad (15)$$

Fig. 3 verifies that our data follow this equation in agreement with previous reports.[59] From the corresponding slopes we receive the values of λ cited also in Table II. We observe that the constant λ of the kinetic Eq. (14) describing the rate of oxygen change upon annealing at 450 °C decreases in the CCz-Si in comparison with the Cz-Si sample and further decreases in the SnCz-Si sample. This reflects the important influence of isovalent impurities on the oxygen aggregation processes in Si. The above behavior may be due to the association of oxygen with the C and Sn in the course of anneals that can affect the kinetics of oxygen loss from solution during the thermal treatment. Notably, it has been determined that the decrease of the annealing temperature from 500 to 450 °C (refer to Fig. 6 of Ref. 51) causes a decrease in the value of λ indicating a similar trend with the effect of the introduction of isovalent dopants of larger size.

Fig. 4 presents the evolution of C versus time for the isothermal anneal at 450 °C for the CCz-Si and SnCz-Si. Obviously the total variation of C in the course of the 224 h isothermal anneal is larger for the case of CCz-Si. It would be interesting to compare the losses of oxygen versus the losses of carbon for these two samples. In order to do that it seems reasonable to find the best fitting curves describing the evolution of oxygen (refer to Fig. 1) and carbon (refer to Fig. 4). From these curves we can calculate the oxygen loss ΔOi and the carbon loss ΔCs for these two samples. Fig. 5 depicts ΔOi versus ΔCs in the course of the 450 °C isothermal anneal. The corresponding slopes (ΔOi/ΔCs) are found to be 2.05 for the CCz-Si sample and 1.55 for the SnCz-Si sample. The first value is in accord with previous reports[3,33] that the loss of carbon and oxygen atom from solution is near the values of two O_i for each C_s. However, for the case of SnCz-Si sample this ratio is substantially lower indicating that additional reactions channels involving oxygen and carbon atoms are activated due to the presence of Sn. Sn is an effective trap for *V*s although C is an effective trap for Si_I and therefore it is expected that when both impurities are present the balance between these primary defects (V, Si_I) to be affected, leading finally to a change of the (ΔOi/ΔCs) ratio.

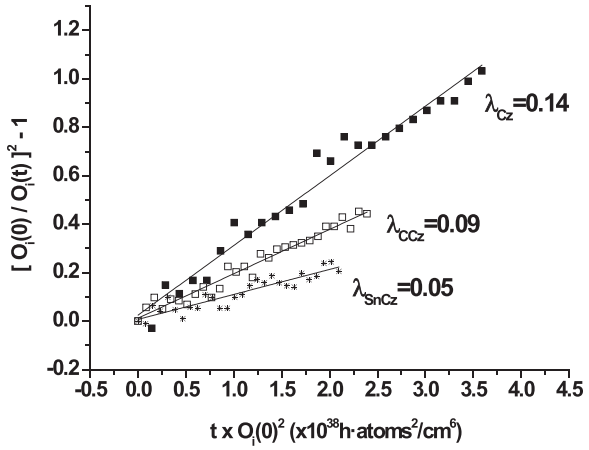

FIG. 3. Plot of $[O_i(0)/O_i(t)]^2-1$ versus $t \times O_i(t)^2$ for the Cz-Si, CCz-Si, and SnCz-Si samples.

B. The effect of Sn on C_sO_i defects

Fig. 6 shows segments of the IR spectra in the region of 560–700 cm^{-1} for the Cz-Si, CCz-Si, and SnCz-Si

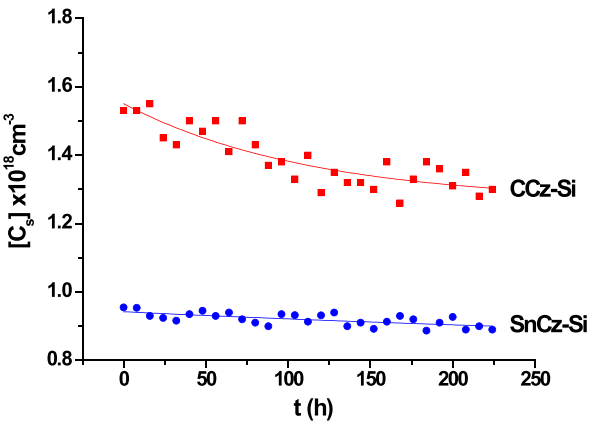

FIG. 4. The evolution of Cs versus annealing time at 450 °C for the CCz-Si and SnCz-Si samples.

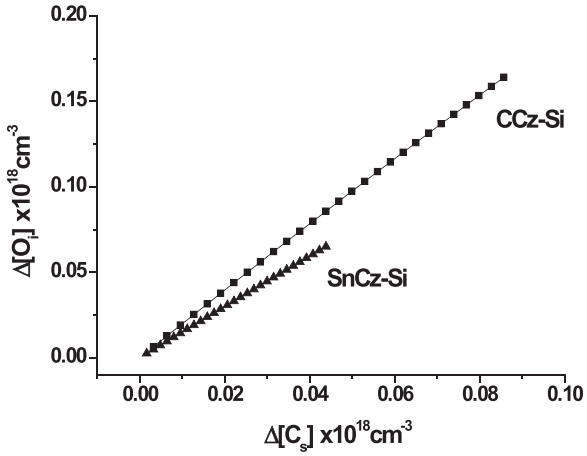

FIG. 5. Oxygen loss ΔOi versus Carbon loss ΔCs from solution as a result of annealing at 450 °C for the CCz-Si and SnCz-Si samples.

samples. Three well-known bands at 683, 636, and 586 cm^{-1} attributed to the C_sO_i defect are seen in the spectra of the CCz-Si sample and also in the SnCz-Si sample. In the latter case the intensity of these bands is significantly lower. The reduction in the formation of the C_sO_i defect indicates that the presence of Sn in the Si lattice affects negatively the association of C and O atoms in the course of annealing. Another possibility could also be that there is the formation of a Sn-C_sO_i related defects something that has not been observed experimentally. In support of this idea DFT calculations indicate that C_sO_i are bound to Sn (refer to Fig. 5 of Ref. 55). Fig. 7 shows the evolution of the 636 cm^{-1} C_sO_i band versus time in the two samples. The other two bands at 586 and 683 cm^{-1} show a similar dependence on the annealing temperature. In the case of the CCz-Si sample the strength of the three bands increases with annealing time stabilized around t = 200 h. In the case of SnCz-Si sample the strength of all the bands is very weak in the whole time of annealing without showing any particular trend.

In Fig. 6, a band at 580 cm^{-1} also appears which is related with TDs.[24,60] Fig. 8 presents the evolution of this band and shows similar behavior with the other TDs bands that will be discussed later.

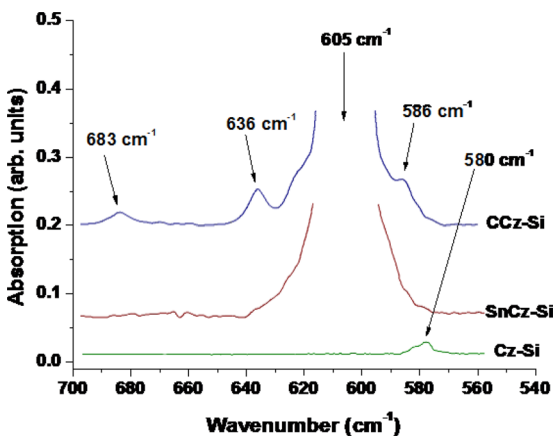

FIG. 6. Segment of IR spectra in the range of 560–700 cm^{-1} for the Cz-Si, CCz-Si, and SnCz-Si samples.

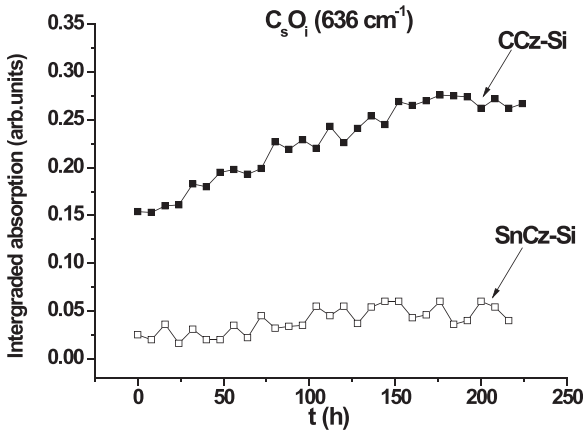

FIG. 7. The evolution of the 636 cm^{-1} C_sO_i band for the CCz-Si and SnCz-Si samples.

C. The effect of C, Sn on TDs

Fig. 9 shows segments of the IR spectra in the region of 980–1040 cm^{-1} for the Cz-Si, CCz-Si, and SnCz-Si samples. The spectra region of 990–1030 cm^{-1} of the Cz-Si sample shows a wide band which evolves upon the annealing. Lorentzian profiling of this region has revealed the presence of three bands at 1000, 1006, and 1012 cm^{-1}. The first two have been previously correlated with TDs and the third with the oxygen dimer defect.[16] On the other hand, these three bands are not present in the spectra of the CCz-Si sample. This was expected since C suppresses the formation of the TDs.[36,39,61] An inspection of the spectra of SnCz-Si reveals the presence of the above bands. Indeed, the two TDs bands at 1000 and 1006 cm^{-1} as well as the oxygen dimer band at 1012 cm^{-1} appear in the spectra but the corresponding signals are very weak in comparison with those of the Cz-Si sample. We note that bands are present in the SnCz-Si sample but absent in the CCz-Si sample. The SnCz-Si sample contains C of about the same order as in the CCz-Si one. It is known that both C[36,39,61] and Sn[49] suppress the formation of thermal donors. However, the mechanisms that govern the reduction of TDs are different for the two cases, as we mentioned above. Carbon introduces tensile strains in the lattice, although Sn compressive ones. The presence of both in Si

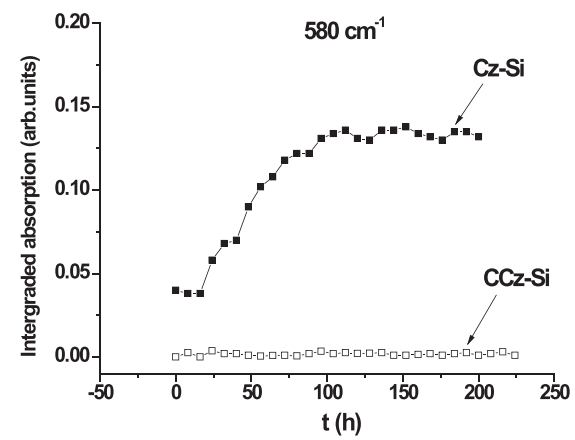

FIG. 8. The evolution of 580 cm^{-1} band vs annealing time at T = 450 °C for the Cz-Si and CCz-Si samples.

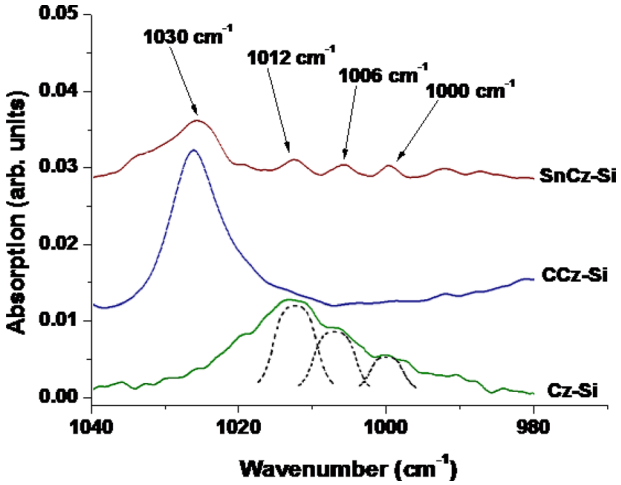

FIG. 9. Segment of IR spectra in the range of 980–1040 cm^{-1} for the Cz-Si, CCz-Si, and SnCz-Si samples.

may lead to a compensation of the strains, moderating the effect of C on the TDs generation and thus allowing a small formation of them, manifested in the IR spectra of the SnCz-Si by the appearance of weak TDs peaks in contrast with the case of CCz-Si. Notably, the three TDs-related bands at 1000, 1006, and 1012 cm^{-1} are very weak in the spectra and therefore, comparison of their intensities between the different samples is difficult. For this reason, we compared the integrated absorption instead of the absorption coefficients of the bands. Fig. 10 shows the evolution of the (a) 1000 and (b) 1012 cm^{-1} bands. The annealing behavior of the 1006 cm^{-1} band is similar to that of 1000 cm^{-1}. The latter two bands attributed to TDs stabilize in strength after ~100 h of anneal at 450 °C, whereas the third band at 1012 cm^{-1} related with the oxygen dimer in Si continue to increase in agreement with previous reports.[16]

Furthermore, a band at 1030 cm^{-1} is also present in the spectra of the CCz-Si sample (Fig. 9). This band is related with the C-O_2 defect[3] and is also present in the spectra of the SnCz-Si sample but weaker. Fig. 11 shows the evolution of the 1030 cm^{-1} band. The reduction in the strength of the band in the SnCz-Si material may be due to similar reasons as we mentioned above for case of the three bands of the C_sO_i defect in the latter material in comparison with the CCz-Si.

Fig. 12 shows segments of the IR spectra in the region of 720–750 cm^{-1} for the Cz-Si, CCz-Si, and SnCz-Si samples. Lorentzian profiling has shown the existence of four bands at 728, 734, 739, and 745 cm^{-1}. Three of these bands at 728, 734, and 745 cm^{-1} has been previously reported[18] and related with the bands at 1000, 1006, and 1012 cm^{-1}, respectively. The bands in the CCz-Si material are very weak. Also the bands are weak in the SnCz-Si material although appear slightly stronger than those in the CCz-Si material showing correspondingly similar behavior with the bands in the frequency range 980–1040 cm^{-1}. This observation supports our previous suggestion that when both C and Sn isovalent dopants are present in the Si lattice the compensation of strains allows for a weak increase of the strength of the TDs bands that is an increase in the formation of the

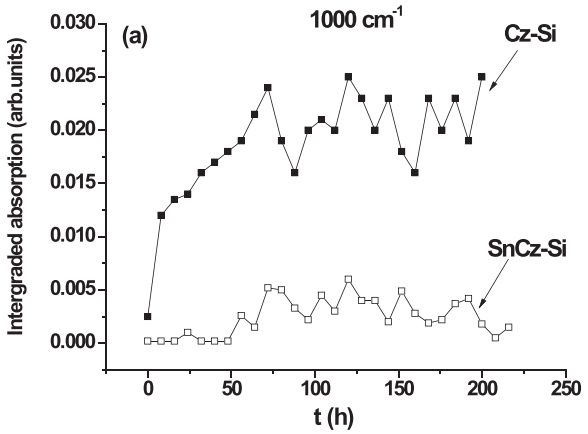

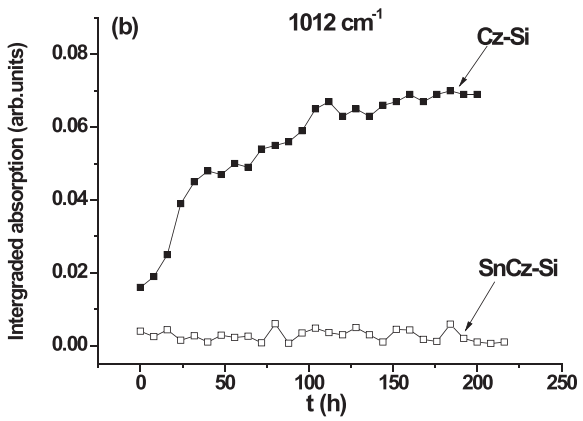

FIG. 10. The evolution of (a) 1000, and (b) 1012 cm^{-1} bands vs annealing time at 450 °C for the Cz-Si and SnCz-Si samples.

TDs. The 734 and 745 cm^{-1} bands were determined to have an annealing behavior similar to that of the 1006 and 1012 cm^{-1} in the Cz-Si samples (Fig. 10) which verifies the connection between the two groups of bands as previously reported.[18] However, the 728 cm^{-1} band shows an anomalous decrease in intensity upon annealing that warrants further investigation.

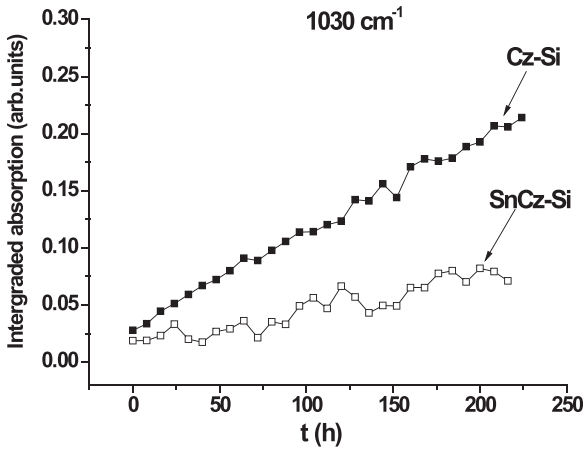

FIG. 11. The evolution of 1030 cm^{-1} band versus annealing time at 450 °C for the CCz-Si and SnCz-Si samples.

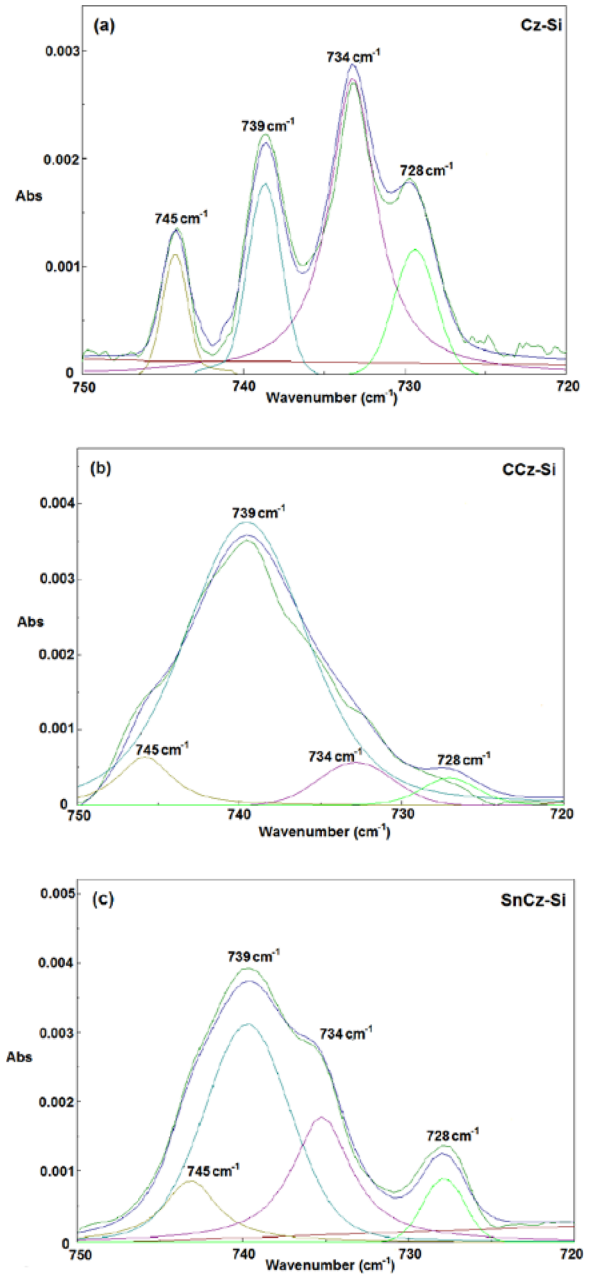

FIG. 12. Segment of IR spectra in the range of 720–750 cm^{-1} for the Cz-Si, CCz-Si, and SnCz-Si samples.

In the present study of the frequency range 720–750 cm^{-1}, an additional band at 739 cm^{-1} is observed in all the samples. This band was not observed previously.[18] Fig. 13 shows the evolution of this band in the Cz-Si, CCz-Si, and SnCz-Si samples. It shows a similar behavior with that of the TDs bands depicted in Figs. 10 and 13. However, the fact that the band appears stronger in the CCz-Si samples is against a correlation with TDs. Importantly, it is known that VO_m complexes serve as precursors for the nucleation of oxide precipitates and such complexes can form in the course of thermal anneals.[62,63] On the other hand, VO_m defect could interact with carbon to form larger clusters. Interestingly, a band at 762 cm^{-1} has been previously correlated with a VO_5C_s structure.[64] Similarly, the 739 cm^{-1} band can be tentatively attributed to a VO_mC_s structure. Furthermore, it is

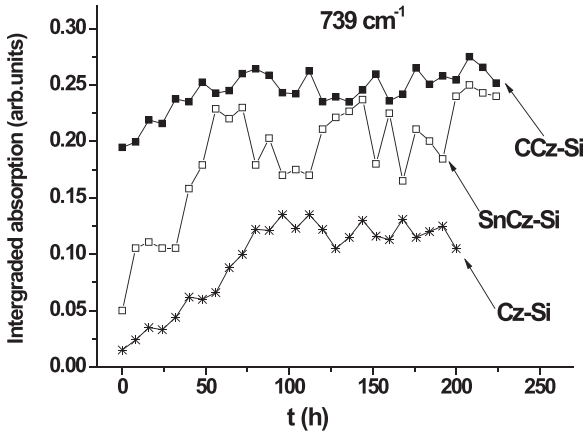

FIG. 13. The evolution of the 739 cm^{-1} band for the Cz-Si, CCz-Si, and SnCz-Si samples.

worth noting that when both C and Sn are present as in the case of the SnCz-Si sample the band appears weaker than in the CCz-Si sample indicating again the effect of the compensation of strains between the two isovalent dopants. This certainly has an influence on the availability of intrinsic defects that is V and Si_I formed in the course of the thermal treatments, which is reflected in the strength of the related bands.

IV. SUMMARY

In the present study, Localized vibrational mode (LVM) spectroscopy was employed to investigate Cz-Si, CCz-Si, and SnCz-Si samples subjected to isothermal anneal at 450 °C. By investigating the impact of C and Sn on the aggregation kinetics of oxygen it is concluded that the reduction rate of oxygen obeys the JMA equation. Here, it is determined that

(1) The activation energy related with the reaction rate constant of the process increases from Cz-Si, to CCz-Si, to SnCz-Si, although the constant λ shows an opposite trend. On the other hand, the time exponent n in the JMA equation is almost equal for the Cz-Si and the CCz-Si samples, although it is reduced in the case of the SnCz-Si sample.

It was further determined that

(2) The presence of Sn suppresses the formation of the C-O defects and this is reflected in the reduction in the strength of the 683, 626, and 586 cm^{-1} bands of C_sO_i defect and the 1030 cm^{-1} band of the $C\text{-}O_2$ defect.
(3) The impact of C and Sn on the formation of TDs is significant. In particular, carbon and Sn suppress the formation of TDs when they are alone in the Si lattice, although the mechanisms are different in the two cases. But when both C and Sn are present, weak TDs peaks appear in the spectra. This can be attributed to the compensation of strains introduced by the two isovalent impurities which tend to mitigate the overall suppression effect leading final to a small formation of TDs. Understandably, C and Sn codoping is not a promising combination for TDs suppression in Si.

[1]C. S. Fuller, N. B. Ditzenberger, N. B. Hannay, and E. Buehler, Phys. Rev. **96**, 833 (1954).
[2]W. Kaiser, Phys. Rev. **105**, 1751 (1957).
[3]A. R. Bean and R. C. Newman, J. Phys. Chem. Solids **33**, 255 (1972).
[4]S. Muller, M. Sprenger, E. G. Sieverts, and C. A. J. Ammerlaan, Solid State Commun. **25**, 987 (1978).
[5]D. Wruck and P. Gaworzewski, Phys. Status Solidi A **56**, 557 (1979).
[6]L. C. Kimerling and J. L. Benton, Appl. Phys. Lett. **39**, 410 (1981).
[7]M. Tajima, U. Gösele, J. Weber, and R. Sauer, Appl. Phys. Lett. **43**, 270 (1983).
[8]B. Pajot, H. Compain, J. Leroueille, and B. Clerjaud, Physica B+C **117–118**, 110 (1983).
[9]G. S. Oehrlein and J. W. Corbett, Mater. Res. Soc. Symp. Proc. **14**, 107 (1983).
[10]M. Stavola, Physica B **146**, 187 (1987).
[11]P. Wagner and J. Hage, Appl. Phys. A **49**, 123 (1989).
[12]C. A. Londos, M. J. Binns, A. R. Brown, S. A. McQuaid, and R. C. Newman, Appl. Phys. Lett. **62**, 1525 (1993).
[13]N. Meilwes, J. M. Spaeth, W. Gotz, and G. Pensl, Semicond. Sci. Technol. **9**, 1623 (1994).
[14]*Oxygen in Silicon, Semiconductor and Semimetals*, edited by F. Shimura (Academic, New York, 1994), Vol. 42.
[15]*Early Stages of Oxygen Precipitation in Silicon*, edited by R. Jones (NATO ASI series, 1996), Vol. 17, and references therein.
[16]J. L. Lindström and T. Hallberg, Phys. Rev. Lett. **72**, 2729 (1994).
[17]J. L. Lindström and T. Hallberg, J. Appl. Phys. **77**, 2684 (1995).
[18]T. Hallberg and J. L. Lindström, J. Appl. Phys. **79**, 7570 (1996).
[19]L. I. Murin, T. Hallberg, V. P. Markevich, and J. L. Lindström, Phys. Rev. Lett. **80**, 93 (1998).
[20]M. Pesola, Y. J. Lee, J. Von Boehm, M. Kauloken, and R. M. Nieminen, Phys. Rev. Lett. **84**, 5343 (2000).
[21]R. Jones, J. Coutinho, S. Öberg, and P. R. Briddon, Physica B **308–310**, 8 (2001).
[22]Y. J. Lee, M. Pesola, J. Von Boehm, and R. M. Nieminen, Phys. Rev. Lett. **86**, 3060 (2001).
[23]Y. J. Lee, J. von Boehm, M. Pesola, and R. M. Nieminen, Phys. Rev. B **66**, 075219 (2002).
[24]J. Coutinho, R. Jones, L. I. Murin, V. P. Markevich, J. L. Lindström, S. Öberg, and P. R. Briddon, Phys. Rev. Lett. **87**, 235501 (2001).
[25]L. I. Murin, J. L. Lindström, V. P. Markevich, A. Misiuk, and C. A. Londos, J. Phys.: Condens. Matter **17**, S2237 (2005).
[26]J. Leroueille, Phys. Status Solidi A **67**, 177 (1981).
[27]R. C. Newman and R. S. Smith, J. Phys. Chem. Solids **30**, 1493 (1969).
[28]G. Davies and R. C. Newman, "Carbon in monocrystalline silicon," in *Handbook in Semiconductors*, edited by S. Mahajan (Elsevier, Amsterdam, 1994), Vol. 3, pp. 1557–1635.
[29]D. Helmreich and E. Sirtl, in *Semiconductor Silicon 1977*, edited by H. R. Huff and E. Sirtl (The Electrochem. Soc. Softbound Ser., Princeton, 1977), p. 626.
[30]P. Gaworzewski and E. Hild, Phys. Status Solidi A **92**, 129 (1985).
[31]U. Gösele, K. Y. Ahn, B. P. R. Marioton, T. Y. Tan, and S. T. Lee, Appl. Phys. A **48**, 219 (1989).
[32]R. C. Newman, A. S. Oates, and F. M. Livingston, J. Phys. C: Solid State Phys. **16**, L667 (1983).
[33]J. L. Lindström, H. Werman, and G. S. Oehrlein, Phys. Status Solidi A **99**, 581 (1987).
[34]R. C. Newman, J. Phys. C: Solid State Phys. **18**, L967 (1985).
[35]P. Deak, L. C. Snyder, and J. W. Corbett, Phys. Rev. B **45**, 11612 (1992).
[36]L. I. Murin and V. P. Markevich, Semiconductors **27**, 108 (1983).
[37]A. Ourmazd, W. Schroter, and A. Bourret, J. Appl. Phys. **56**, 1670 (1984).
[38]U. Gösele and T. Y. Tan, Appl. Phys. A **28**, 79 (1982).
[39]L. I. Murin and V. P. Markevich, Mater. Sci. Forum **196–201**, 1315 (1995).
[40]X. Yu, J. Chen, X. Ma, and D. Yang, Mater. Sci. Eng. R **74**, 1 (2013).
[41]G. D. Watkins, Phys. Rev. B **12**, 4383 (1975).
[42]M. Fanciulli and J. R. Byberg, Physica B **273–274**, 524 (1999); A. Chroneos, E. N. Sgourou, C. A. Londos, and U. Schwingenschlögl, Appl. Phys. Rev. **2**, 021306 (2015); A. Chroneos and C. A. Londos, J. Appl. Phys. **107**, 093518 (2010).
[43]Yu. V. Pomozov, M. G. Sosnin, L. I. Khirunenko, and V. I. Yashnik, Semiconductors **34**, 994 (2000).
[44]V. B. Neimash, A. Kraitchinskii, M. Kras'ko, O. Puzenko, C. Clays, E. Simoen, B. Svensson, and A. Kuznetsov, J. Electrochem. Soc. **147**, 2727 (2000).
[45]W. Wijaranacula, J. Appl. Phys. **69**, 2737 (1991); A. Chroneos, C. A. Londos, E. N. Sgourou, and P. Pochet, Appl. Phys. Lett. **99**, 241901 (2011); A. Chroneos, Phys. Stat. Sol. B **244**, 3206 (2007).
[46]Yu. M. Batitskii, N. I. Gorbacheva, P. M. Grinshtein, M. A. Il'in, V. P. Kuznetsov, M. G. Mil'vidskii, and B. M. Turovskii, Sov. Phys. Semicond. **22**, 187 (1988).
[47]W. Kaiser, H. L. Frisch, and H. Reiss, Phys. Rev. **112**, 1546 (1958).
[48]A. Brelot, IEEE Trans. Nucl. Sci. **19**, 220 (1972).
[49]A. Baghdadi, W. M. Bullis, M. C. Choarkin, Y.-Z. Li, R. I. Seace, R. W. Series, P. Stallhofer, and M. Watanabe, J. Electrochem. Soc. **136**, 2015 (1989).
[50]J. L. Regolini, J. P. Stoquert, C. Ganter, and P. Sifferty, J. Electrochem. Soc. **133**, 2165 (1986).
[51]H. Yamanaka, J. Appl. Phys. **33**, 3319 (1994).
[52]R. A. Craven, *Semiconductor Silicon 1981*, edited by H. R. Huff, R. J. Kriegler, and Y. Takeishi (Electrochemical Society, Pennington, 1981), p. 273.
[53]J. Burke, *The Kinetics of Phase Transformation in Metals* (Pergamon, London, 1965), Chap. 7.
[54]C. Clays, E. Simoen, V. B. Neimash, A. Kraitchinskii, M. Kras'ko, O. Puzenko, A. Blondeel, and P. Clauws, J. Electrochem. Soc. **148**, G738 (2001).
[55]A. Chroneos, C. A. Londos, and E. N. Sgourou, J. Appl. Phys. **110**, 093507 (2011).
[56]E. N. Sgourou, D. Timerkaeva, C. A. Londos, D. Aliprantis, A. Chroneos, D. Caliste, and P. Pochet, J. Appl. Phys. **113**, 113506 (2013).
[57]C. Gao, X. Ma, and D. Yang, Phys. Status Solidi A **210**, 2199 (2013).
[58]H. Wang, A. Chroneos, C. A. Londos, E. N. Sgourou, and U. Schwingenschlögl, Phys. Chem. Chem. Phys. **16**, 8487 (2014).
[59]M. P. Guse and R. Kleinhenz, J. Appl. Phys **72**, 4615 (1992).
[60]J. L. Lindström and T. Hallberg, *Early Stages of Oxygen Precipitation in Silicon*, edited by R. Jones (NATO ASI series, 1996), Vol. 17, p. 41.
[61]R. C. Newman, in Oxygen, Carbon, Hydrogen and Nitrogen in Crystalline Silicon, edited by J. C. Mikkelsen, Jr., S. J. Pearton, J. W. Corbett, and S. J. Pennycook (MRS, Pittsburgh, PA, 1986), Vol. 59, p. 403.
[62]V. V. Voronkov and R. Falster, J. Electrochem. Soc. **149**, G167 (2002).
[63]P. Dong, J. Zhao, X. B. Liang, D. X. Tian, S. Yuan, X. G. Yu, X. Y. Ma, and D. R. Yang, J. Appl. Phys. **117**, 025705 (2015).
[64]C. A. Londos, D. Aliprantis, E. N. Sgourou, A. Chroneos, and P. Pochet, J. Appl. Phys. **111**, 123508 (2012).